A STUDY OF APPROPRIATE ARRANGEMENT OF THERMOELASTIC ACTUATOR

I. Doležel[1)], M. Donátová[2)], P. Karban[2)], B. Ulrych[2)]

[1)]*Department of Electrical Power Engineering, Faculty of Electrical Engineering, CTU, Technická 2,166 27 Prague, Czech Republic, tel.: +420 224353941. E-mail: dolezel@fel.cvut.cz*

[2)]*Department of Theory of Electrical Engineering, Faculty of Electrical Engineering, UWB, Univerzitní 26,306 14 Pilsen, Czech Republic, tel.: +420 377634631. E-mail: donatm, karban, ulrych}@kte.zcu.cz*

Summary: The actuators working on the principle of thermoelasticity belong to novel elements of this kind that are characterized by very high forces acting at relatively low shifts of the dilatation element. The paper analyses their operation properties in the dependence of selected geometrical parameters of the device and also the amplitude and frequency of the field current. The task is solved as a coupled electromagnetic-thermoelastic problem. The theoretical considerations are illustrated on an example whose results are discussed.

1. INTRODUCTION

The actuators are devices transforming electric energy into mechanical motion or forces. They are widely spread in a great deal of industrial, transport, control and other systems. Every actuator usually consists of several static and movable parts. While the static parts form its body and primary electric circuit (but there are exceptions), the movable parts are intended for transferring the force effects.

Operation of the actuators is derived from several physical principles. We can mention electromagnetic and electrodynamic force effects, magnetostriction, piezoelectricity etc. All these principles have been known for many years and relevant information about them can be found in several books and numerous journal references (see, for example, [1]–[3]).

The characteristics and properties of particular types of the actuators cover quite a broad domain. Nevertheless, the situation becomes to be problematic when we need to reach high forces at small shifts. A typical application is depicted in Fig. 1, where four actuators hold a metal body that is to be machined.

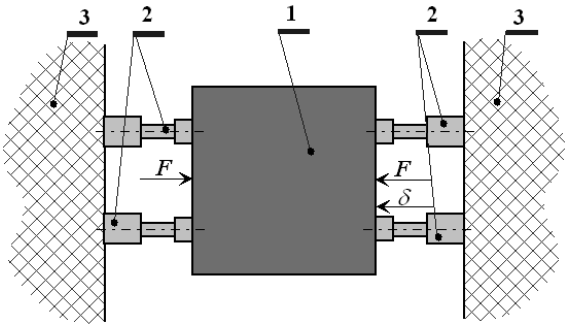

1 - fixed body, **2** - fixing actuators, **3** - stiff frame

Fig. 1. Four actuators holding a metal body

The classical actuators, unfortunately, are not able to satisfy such a condition. Their main drawback is that the forces they can reach are by several orders smaller than necessary. That is why the authors started investigating a new class of these devices based on thermoelasticity. Their principle follows from Fig. 2. Its arrangement is assumed (with a small inaccuracy) axisymmetric.

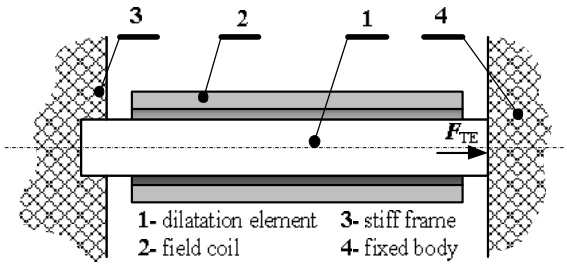

Fig. 2. Schematic view of the thermoelastic actuator

The steel dilatation element **1** clamped in a stiff wall **3** is heated by the field coil **2** carrying harmonic current of a given amplitude and frequency. The Joule and magnetization losses in it bring about its temperature rise and thermoelastic strains and stresses. These strains result in the total force $\boldsymbol{F}_{\mathrm{TE}}$ acting on the fixed body **4** that depend on the stiffness of the whole system. The smaller displacement δ (Fig. 1) the higher force $\boldsymbol{F}_{\mathrm{TE}}$ and vice versa. In order to avoid its plastic deformation the maximum mechanical stress in the dilatation element must not exceed the limit of elasticity of the used steel material.

The force $\boldsymbol{F}_{\mathrm{TE}}$ depends on a number of various factors. In works [4] and [5] the authors investigated the dependence of its value particularly on the amplitude of the field current and its frequency. But it also depends on the length of the dilatation element and its cross-section. In fact, this force grows approximately linearly with the length of the element and in this way we seemingly could obtain any desired value. On the other hand, such a growth of the length could result in the loss of axial stability of the device. And this is a contradiction leading to the necessity of an appropriate compromise.

The paper presents a methodology of finding the most important characteristics of the device as functions of the geometry of the dilatation element. In this sense it represents a natural continuation of the above papers [4] and [5].

2. CONTINUOUS MATHEMATICAL MODEL

The task generally represents a nonlinear coupled problem characterized by the interaction of the electromagnetic field, field of temperature and field of thermoelastic displacements. Every field is described by a partial differential equation (PDE) whose coefficients are given by expressions containing the physical parameters of the material. Unfortunately, as these physical parameters vary with the growing temperature, the coefficients are not constant and must be properly adjusted in the course of computation.

Another problem often consists in the fact, that the problem has also contact character. The dilatation element first touches the fixed body first by quite a small surface in the form of a circular ring whose area then gradually grows with the growing temperature. This may brings difficulties in determination of the time evolution of the forces acting on the body.

The electromagnetic field is solved independently of the other two fields. This means that the electrical conductivity and magnetic permeability of the material involved do not depend on the temperature. But this simplification has practically no negative influence on the results because the temperature of the system is supposed not to exceed about 300 °C.

The distribution of the electromagnetic field in space and time is (because of the presence of the nonlinear dilatation element) described by the solution of the well-known parabolic PDE for the magnetic vector potential $\boldsymbol{A}$ in the form [6]

$$\operatorname{curl}\left(\frac{1}{\mu}\operatorname{curl}\boldsymbol{A}\right)+\gamma\frac{\partial\boldsymbol{A}}{\partial t}=\boldsymbol{J}_{\mathrm{ext}} \tag{1}$$

where μ denotes the magnetic permeability, γ the electric conductivity and $\boldsymbol{J}_{\mathrm{ext}}$ the vector of the external current density in the field coil.

But solution to this equation is, in this case, practically unfeasible due to relatively long time of the process of heating (usually of the order of seconds or tens of seconds). That is why the model was simplified considering the magnetic field harmonic. Then it can be described by the Helmholtz equation for the phasor $\underline{\boldsymbol{A}}$ of the magnetic vector potential $\boldsymbol{A}$

$$\operatorname{curlcurl}\underline{\boldsymbol{A}}+\mathrm{j}\cdot\omega\gamma\mu\underline{\boldsymbol{A}}=\mu\underline{\boldsymbol{J}}_{\mathrm{ext}} \tag{2}$$

The magnetic permeability μ in every element is considered constant, but its value is not known in advance. Finding its corresponding values requires an appropriate iterative process and the value of permeability in all cells at every iteration step must be adjusted to the relevant magnetic flux density.

This simplification is also advantageous from the viewpoint of determining the distribution of the specific losses w representing the internal sources of heat in ferromagnetic dilatation element **1** (Fig. 2). These losses are considered as a sum of the specific Joule losses w_{J} and magnetization losses w_{m}, so that

$$w=w_{\mathrm{J}}+w_{\mathrm{m}} \tag{3}$$

where

$$w_{\mathrm{J}}=\frac{\left|\underline{\boldsymbol{J}}_{\mathrm{eddy}}\right|^2}{\gamma},\quad \underline{\boldsymbol{J}}_{\mathrm{eddy}}=\mathrm{j}\cdot\omega\gamma\underline{\boldsymbol{A}} \tag{4}$$

while w_{m} are determined from the known loss dependence $w_{\mathrm{m}}=w_{\mathrm{m}}\left(\left|\underline{\boldsymbol{B}}\right|\right)$ for the used material (magnetic flux density $\boldsymbol{B}$ in every element is in this model also harmonic).

The boundary conditions along the axis of the arrangement and artificial boundary placed at a sufficient distance from the system are of the Dirichlet type.

The temperature and stress-strain fields should be solved in the hard-coupled formulation. Nevertheless, as we investigate only the steady states, only a small error appears when using the operator-splitting method and solving both fields separately (another case would be the solution of the nonstationary problem, where disregarding the mutual links could lead to a substantial loss of accuracy).

The distribution of the steady-state temperature field is described by equation [7]

$$\operatorname{div}\left(\lambda\cdot\operatorname{grad}T\right)=-w \tag{5}$$

where λ is the thermal conductivity (a temperature-dependent function) and w the internal sources of heat given by (3). The boundary conditions generally respect the convection of heat from the shell of the device into ambient air and radiation.

The solution of the thermoelastic problem may be carried out by several different ways. We will mention four fundamental approaches that are based on

- the Lamé equation for the displacements,
- the standard equations based on the balance of forces in an elementary volume of the continuum,
- the Airy function or
- the variational principle.

After some considerations we used the Lamé equation that reads

$$\begin{aligned}&\left(\varphi+\psi\right)\cdot\operatorname{grad}\left(\operatorname{div}\boldsymbol{u}\right)+\psi\cdot\Delta\boldsymbol{u}-\\&-\left(3\varphi+2\psi\right)\cdot\alpha_{\mathrm{T}}\cdot\operatorname{grad}T+\boldsymbol{f}=\boldsymbol{0},\end{aligned} \tag{6}$$

where φ,ψ are coefficients associated with material parameters by relations [8]

$$\varphi=\frac{\nu\cdot E}{\left(1+\nu\right)\left(1-2\nu\right)},\ \psi=\frac{E}{2\cdot\left(1+\nu\right)}. \tag{7}$$

Here E denotes the Young modulus of elasticity and ν the Poisson coefficient of the transverse con-

traction. Finally $\boldsymbol{u} = (u_r, u_\varphi, u_z)$ represents the displacement vector, α_T the coefficient of linear thermal dilatability and $\boldsymbol{f}$ the vector of internal mechanical volume forces.

The boundary conditions follow from the assumption that the left front of the device (Fig. 2) is fixed.

The knowledge of the displacement is the starting point for finding the corresponding deformations. These can be calculated (in the cylindrical coordinate system r, z, φ) from formulas

$$\varepsilon_{rr} = \frac{\partial u_r}{\partial r},\ \varepsilon_{\varphi\varphi} = \frac{u_r}{r} + \frac{1}{r}\cdot\frac{\partial u_\varphi}{\partial \varphi},\ \varepsilon_{zz} = \frac{\partial u_z}{\partial z},$$
$$\varepsilon_{r\varphi} = \frac{1}{2}\left(\frac{1}{r}\cdot\frac{\partial u_r}{\partial \varphi} + \frac{\partial u_\varphi}{\partial r} - \frac{u_\varphi}{r}\right), \qquad (8)$$
$$\varepsilon_{rz} = \frac{1}{2}\left(\frac{\partial u_r}{\partial z} + \frac{\partial u_z}{\partial r}\right),\ \varepsilon_{\varphi z} = \frac{1}{2}\left(\frac{\partial u_\varphi}{\partial z} + \frac{1}{r}\cdot\frac{\partial u_z}{\partial \varphi}\right).$$

Using the Hook law in the tensorial form we finally calculate the corresponding strains and stresses in shell **1** that is, from the mechanical viewpoint, the most exposed part of the device.

The axial component $F_{TE,z}$ of the total force $\boldsymbol{F}_{TE}$ acting in the dilatation element in the direction of axis z (for the given displacement) then follows from the integration of the relevant axial stresses over its cross-section. There holds

$$F_{TE,z} = \iint_{S_{1,4}} \sigma_{zz}\,\mathrm{d}S, \qquad (9)$$

σ_{zz} denoting the distribution of the axial stresses in the dilatation element **1** along its contact with the fixed body **4** (see Fig. 2), whose area is $S_{1,4}$.

3. ILLUSTRATIVE EXAMPLE

The aim of the example is the qualitative evaluation of basic aspects influencing the operation parameters of the actuator – the maximum thermoelastic force $F_{TE,z,max}$ and maximum shift $\Delta u_{z,max}$ of its dilatation element **1**. The basic arrangement of the actuator is depicted in Fig. 3. Its starting length $l_{00} = 0.145$ m and starting radius $r_{00} = 0.015$ m. The detailed information about the physical parameters of its structural parts is listed in Tab. 1. The magnetization characteristic of the dilatation element (steel 12040) is depicted in Fig. 4. The relative magnetic permeability of other parts μ_r is equal to 1.

The main parameters that affect the operation of the actuators are:

- the real length l_{0i} and radius r_{0i} of the dilatation element **1** (during the computations we considered $l_{0i} = 1.1\cdot l_{00}, 1.2\cdot l_{00}, 1.3\cdot l_{00}$ with $r_{0i} = r_{00}$ and $r_{0i} = 1.1\cdot r_{00}, 1.2\cdot r_{00}, 1.3\cdot r_{00}$ with $l_{0i} = l_{00}$),
- the amplitude of the current density $\boldsymbol{J}_{ext}$ (with only one nonzero component J_φ in the tangential direction) of the field current I_{ext} and
- frequency f of the field current.

These aspects are discussed in the next paragraphs.

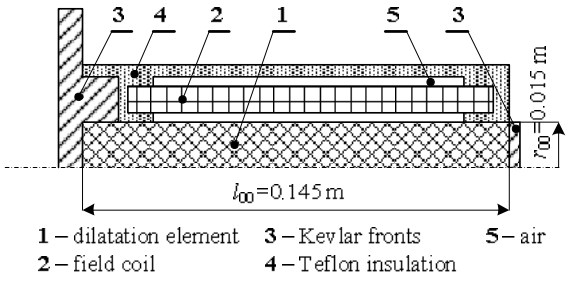

Fig. 3. The starting arrangement of the investigated actuator with principal dimensions

Table 1

Basic physical parameters of the structural parts of the actuator [9], [10]

material position in Fig. 3	γ (S/m)	λ (W/mK)	E (N/m^2)	υ (–)	α_T (1/K)
steel 12 040 **1**	$5\cdot10^6$	$^*\lambda(T)$	$2.1\cdot10^{11}$	0.3	$1.25\cdot10^{-5}$
Kevlar **3**	0.04	1.0	$1.24\cdot10^{11}$	0.1	$2\cdot10^{-6}$
Teflon **4**	0	1.6	–	–	–
copper **2**	$^{**}5.7\cdot10^7$	306.1	–	–	–

$^*\lambda(T)$ see Fig. 5

** the specific conductivity of copper has to be reduced by the coefficient of filling of the coil whose value is 0.785 (the coil is wound by a conductor of circular cross-section). Therefore, it is necessary to consider $\gamma_{Cu} = 4.474\cdot10^7$ S/m.

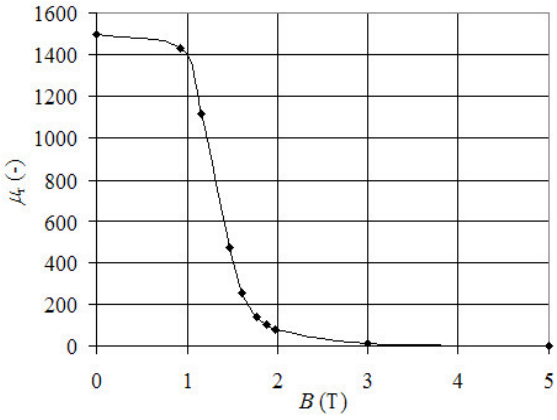

Fig. 4. Dependence $\mu_r = \mu_r(B)$ for carbon steel 12 040

The results presented in the next paragraphs were obtained by the numerical solution of the problem by means of the FEM-based code QuickField [11] and several own procedures. Solved were equations (2), (5) and (6). The temperature field was calculated

only with the boundary condition of convection. Radiation was neglected because the external boundary is cold (the thermal conductivity of Teflon and Kevlar insulating parts is very low).

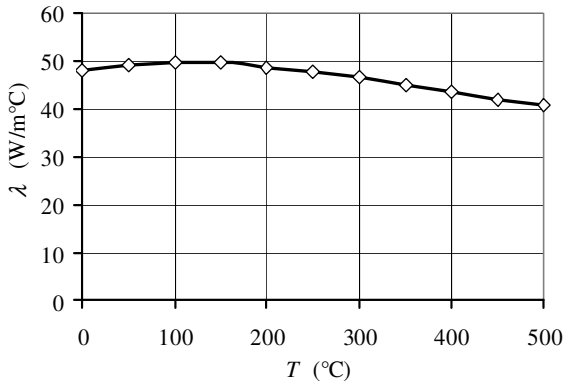

Fig. 5. Dependence $\lambda = \lambda(T)$ *for carbon steel* 12 040

All three fields were checked with respect to the convergence of results. We used discretization meshes with about

- 190000 nodes for the magnetic field,
- 80000 nodes for the temperature field,
- 25000 nodes for the field of displacements.

Figs. 6–9 show some selected results for the starting arrangement of the actuator (see Fig. 3).

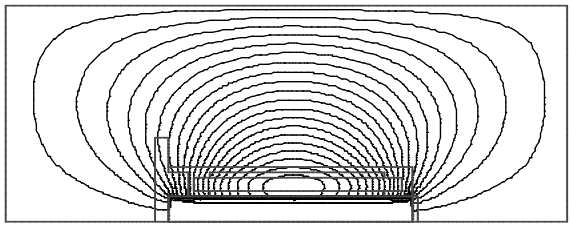

Fig. 6. Electromagnetic field of the actuator (starting arrangement, $J_\varphi = 2\,A/mm^2$, $f = 50\,Hz$)

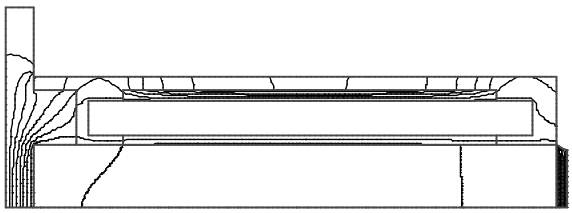

Fig. 7. Stationary temperature field of the actuator (starting arrangement, $J_\varphi = 2\,A/mm^2$, $f = 50\,Hz$, $T_{max} = 68.2\,°C$, $T_{min} = 20.0\,°C$)

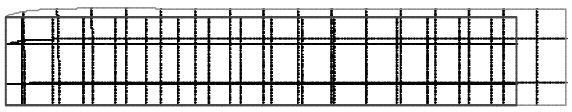

Fig. 8. Field of thermoelastic displacements of the actuator (starting arrangement, $J_\varphi = 2\,A/mm^2$, $f = 50\,Hz$, *maximum displacement* $\Delta u_{z,max} = 8.74 \cdot 10^{-5}\,m$, $F_{TE,z,min} = 0$)

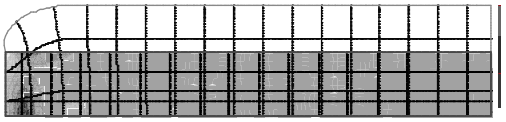

Fig. 9. Field of thermoelastic displacements of the actuator (starting arrangement, $J_\varphi = 2\,A/mm^2$, $f = 50\,Hz$, *minimum displacement* $\Delta u_{z,min} = 0\,m$, $F_{TE,z,max} = 88.285\,kN$)

The most important results representing the main contribution of the paper follow from Figs. 10a–13b. On their basis we can draw these conclusions:

The specific Joule losses w_J (see Figs. 10a, 10b) in the dilatation element **1** grow both with growing frequency f of the field current and (even more expressively) with growing amplitude of its density J_φ. These losses also grow with the length l_{0i} of the dilatation element while the growth of its radius r_{0i} leads to their reduction. The reason of such a behavior consists in the fact that the domain of the dilatation element with induced eddy currents is larger in case of longer, thinner element than in case of shorter, but thicker cylinder (its volume is considered constant).

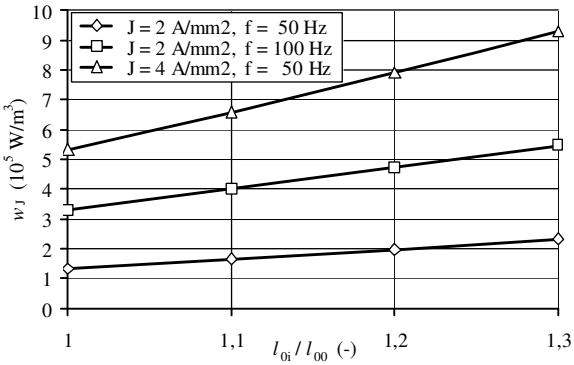

Fig. 10a. Dependence of the specific Joule losses w_J *in the dilatation element* **2** *on this length* l_{0i} ($l_{00} = 0.145\,m$, $r_{0i} = r_{00} = 0.015\,m$)

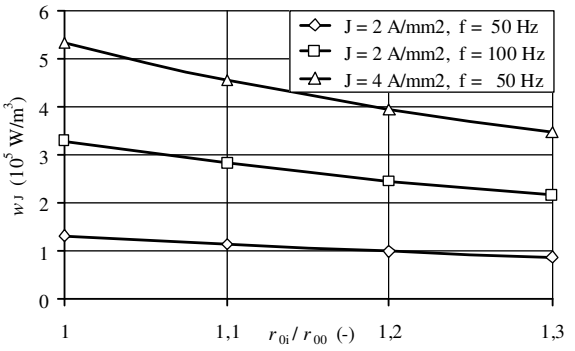

Fig. 10b. Dependence of the specific Joule losses w_J *in the dilatation element* **2** *on this radius* r_{0i} ($r_{00} = 0.015\,m$, $l_{0i} = l_{00} = 0.145\,m$)

The average temperatures $T_{\mathrm{de,a}}$ of the dilatation element **1** and maximum temperatures $T_{\mathrm{c,max}}$ in the field coil **2** as functions of the geometry of the element **1** are depicted in Figs. 11a and 11b. They grow again with increasing frequency f of the field current and, even more expressively, with growing amplitude of its density J_φ (the growth is sometimes so high that it even exceeds the acceptable limit ≈ 250 °C, compare Fig. 11a). This is evidently caused by the corresponding evolution of the specific Joule losses w_{J}. The growth is again supported by growth of the length l_{0i} of the dilatation element **1** and suppressed by growth of its radius r_{0i}. In this case smaller amount of heat (compare the losses w_{J} in Figs. 10a, 10b) produced within the surface layer of shorter length does not heat up the "deeper" layers of the dilatation cylinder of greater radius.

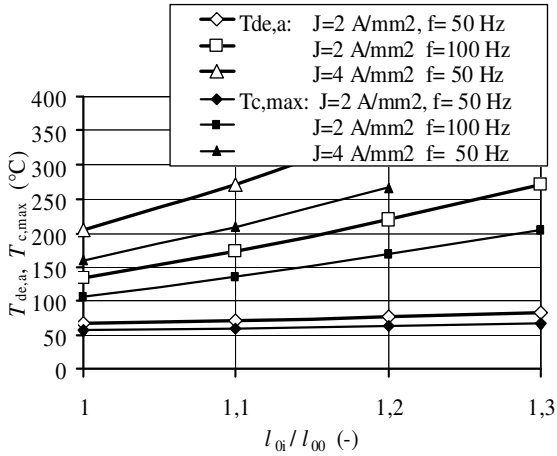

Fig. 11a. Dependence of the average temperature $T_{de,a}$ of the dilatation element **1** *and maximum temperature $T_{c,\max}$ of the field coil* **2** *on the length l_{0i} of element* **1** *($l_{00} = 0.145\,m$, $r_{0i} = r_{00} = 0.015\,m$)*

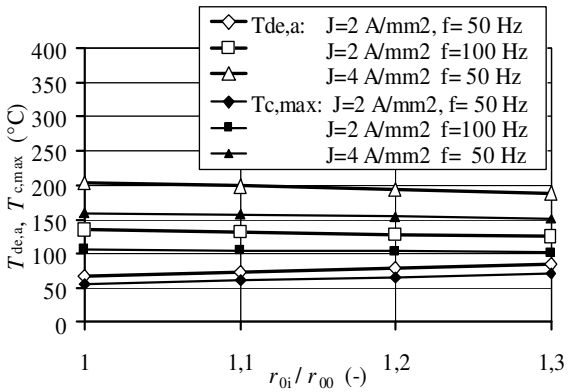

Fig. 11b. Dependence of the average temperature $T_{de,a}$ of the dilatation element **1** *and maximum temperature $T_{c,\max}$ of the field coil* **2** *on the radius r_{0i} of element* **1** *($r_{00} = 0.015\,m$, $l_{0i} = l_{00} = 0.145\,m$)*

The maximum thermoelastic forces $F_{\mathrm{TE},z,\max}$ produced by the dilatation element **1** as functions of its geometry are shown in Figs. 12a and 12b. They grow with the frequency f of the field current, with the amplitude of its density J_φ, with its length l_{0i} (which is given by the corresponding growth of temperature $T_{\mathrm{de,a}}$, compare Fig. 11a) and finally even with its radius r_{0i}. The last case shows that this growth (even when small) at practically not increasing temperatures $T_{\mathrm{de,a}}$, compare Fig. 11b, follows from the fact that smaller thermoelastic stresses σ_{zz} proportional to $T_{\mathrm{de,a}}$ act on larger cross-section of the dilatation element **1** growing with r_{0i}^2.

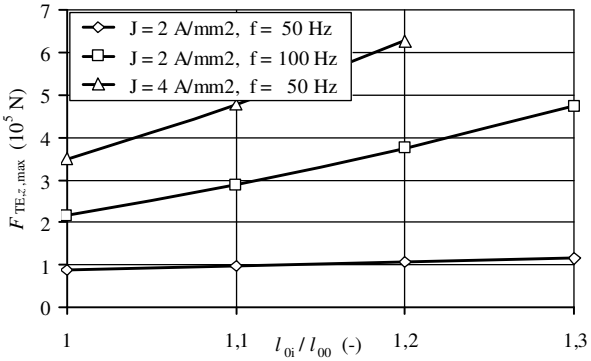

Fig. 12a. Dependence of the maximum thermoelastic force $F_{TE,z,\max}$ on the length l_{0i} of element **1** *($l_{00} = 0.145\,m$, $r_{0i} = r_{00} = 0.015\,m$)*

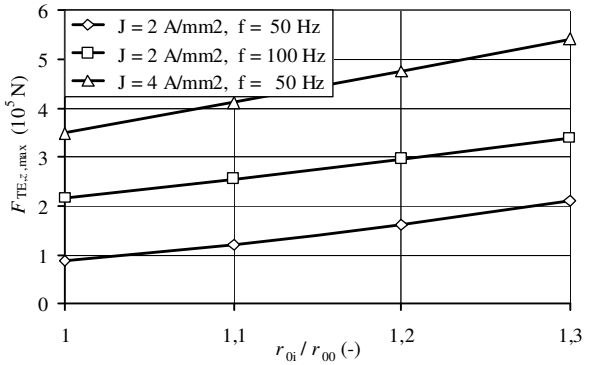

Fig. 12b Dependence of the maximum thermoelastic force $F_{TE,z,\max}$ on the radius r_{0i} of element **1** *($r_{00} = 0.015\,m$, $l_{0i} = l_{00} = 0.145\,m$)*

The maximum thermoelastic displacements $\Delta u_{z,\max}$ of the dilatation element **1** as functions of its geometry are shown in Figs. 13a and 13b. They also grow with the frequency f of the field current, with the amplitude of its density J_φ. But unlike the thermoelastic forces $F_{\mathrm{TE},z,\max}$ the growth is supported only by the increase of the length l_{0i} of the dilatation element **1**. Here the variations of the ra-

dius r_{0i} do not have practically any influence. It can be explained by the following considerations:

- In the first case the effects of growth of the length l_{0i} of element **1** and growth of the temperature $T_{\mathrm{de,a}}$ superimpose (compare Fig. 11a).
- In the second case no growth of the temperature $T_{\mathrm{de,a}}$ appears with the growth of the radius r_{0i} (compare Fig. 11b). And the growth of radius r_{0i} itself does not influence its dilatation in the axial direction.

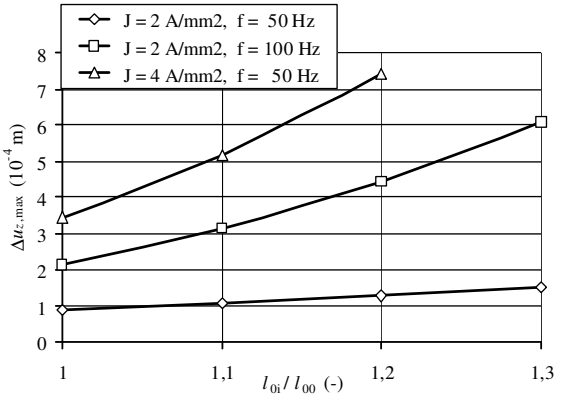

Fig. 13a. Dependence of the maximum thermoelastic displacement $\Delta u_{z,max}$ on the length l_{0i} of element **1**

($l_{00} = 0.145\,m$, $r_{0i} = r_{00} = 0.015\,m$)

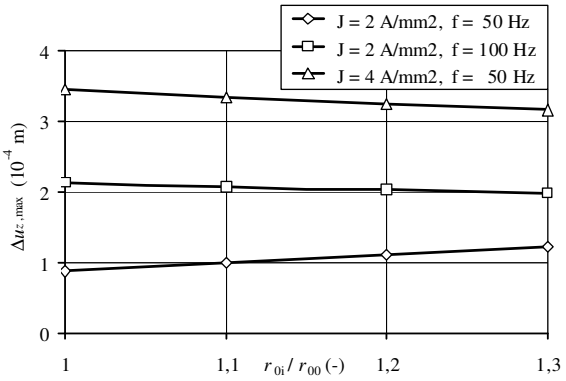

Fig. 13b. Dependence of the maximum thermoelastic displacement $\Delta u_{z,max}$ on the radius r_{0i} of element **1**

($r_{00} = 0.015\,m$, $l_{0i} = l_{00} = 0.145\,m$)

4. CONCLUSION

Evidently, the thermoelastic actuators are devices that are able to produce very high forces and may be used for specific industrial applications such as fixing various bodies. The authors see their further improvement in using intelligent materials with highly developed pseudoplasticity.

Important is also their dynamic behavior (in selected applications the time of producing the force may be of great importance). That is why the authors will continue in their research.

Acknowledgement

The Financial support of the Research Plans MSM6840770017 and grant project GA ČR 102/07/0496 is gratefully acknowledged.

REFERENCES

[1] Janocha, H.: *Actuators, Basics & Applications.* Springer & NY Inc, 2004.

[2] Busch-Vishniac, I.J.: *Electromechanical sensors and actuators.* Springer Verlag Berlin, 1998.

[3] Brauer, J.R.: *Magnetic actuators and sensors.* John Wiley & Sons, 2006.

[4] Doležel, I., Karban, P., Ulrych, B., Pantelyat, M., Matyukhin, M., Gontarowskiy, P.: *Numerical Model of a Thermoelastic Actuator Solved as a Coupled Contact Problem.* COMPEL 2007, Vol. 36, No. 4, pp. 1063–1072.

[5] Doležel, I., Karban, P., Ulrych, B., Pantelyat, M., Matyukhin, M., Gontarowskiy, P., Shulzhenko, M.: *Limit Operation Regimes of Actuators Working on Principle of Thermoelasticity.* Proc. COMPUMAG 2007, Aachen, Germany, 24–28. 6. 2007, Accepted to IEEE Trans. Mag. 2008.

[6] Stratton, J.: *Electromagnetic Theory*. McGraw Hill, 1941.

[7] Holman, J.P.: *Heat Transfer*. McGraw Hill, 2002.

[8] Boley, B., Wiener, J.: *Theory of Thermal Stresses*. NY, 1960.

[9] Mikulcak, J. et al.: *Mathematical, Physical and Chemical Tables*. SPN, Prague, 1970 (in Czech).

[10] www. azom.com.

[11] www.quickfield.com.